

MADPH-98-1072
hep-ph/9808299
August, 1998

TWO-LOOP EFFECTIVE POTENTIAL CALCULATION OF THE LIGHTEST CP -EVEN HIGGS-BOSON MASS IN THE MSSM

REN-JIE ZHANG*

*Department of Physics
University of Wisconsin
1150 University Avenue
Madison, Wisconsin 53706 USA*

Abstract

We calculate a two-loop effective potential to the order of $\mathcal{O}(\lambda_t^2 \alpha_s)$ in the MSSM. We then study the corresponding two-loop corrections to the CP -even Higgs-boson mass for arbitrary $\tan \beta$ and left-right top-squark mixings. We find that the lightest Higgs-boson mass is changed by at most a few GeV. We also show the improved scale dependence and compare to previous two-loop analyses.

*rjzhang@pheno.physics.wisc.edu

1 Introduction

In the minimal supersymmetric standard model (MSSM), the Higgs sector is composed of three neutral (two CP -even, one CP -odd) and two charged scalar bosons. An important fact of the model is that the quartic self-coupling of the lightest CP -even Higgs boson h is not a free parameter, but related to the standard model gauge couplings g and g' ; as a result, the Higgs boson has an upper bounded tree-level mass, $m_h \leq M_Z$. This limit, however, is violated when the one-loop radiative corrections are included.

The well-known dominant one-loop radiative correction comes from the incomplete cancellation of the virtual top-quark and top-squark loops [1], it approximately has the size $\Delta m_h^2 \simeq \frac{3\lambda_t^2 m_t^2}{4\pi^2} \log(m_{\tilde{t}}^2/m_t^2)$. Taking $m_{\tilde{t}} = 100 - 1000$ GeV, one finds a large correction, $\Delta m_h \simeq$ a few $- 50$ GeV, due to the relatively large top-quark mass $m_t^{\text{pole}} = 175$ GeV. The one-loop Higgs-boson mass sensitively depends on the top-quark mass, and generally varies with the change of renormalization scale. So it remains a quite important problem to study the magnitude of two-loop radiative corrections and the scale dependence of the Higgs-boson mass after these corrections.

There are basically two approaches to calculate the two-loop radiative corrections. In the renormalization group equation (RGE)-improved effective potential approach [2, 3, 4], one uses the one-loop effective potential, together with two-loop RGEs, then all leading-order and next-to-leading-order corrections can be calculated. The finite one-loop threshold corrections arising from the decouplings of the heavy top-squarks have also been included, both for the small and large left-right top-squark mixings. It is further observed that by judiciously setting the renormalization scale, one can use the one-loop renormalized Higgs-boson mass as a good approximation to the full two-loop results [3, 5].

The second approach involves a two-loop effective potential. In the special case of $\tan \beta \rightarrow \infty$ and no left-right mixing in the top-squark sector, Hempfling and Hoang have calculated the upper bound to the two-loop Higgs-boson mass [6]. Their results qualitatively agree with the previous approach. Recently, two-loop corrections to m_h have also been computed by an explicit diagrammatic method [7].

It is the purpose of this paper to generalize the two-loop effective potential calculation of [6] to the case of arbitrary $\tan \beta$ and left-right top-squark mixings. The effective potential method has an advantage over other approaches because it is simple and does not require complicate programming. In this paper we will study the improved scale dependence of the Higgs-boson mass m_h and the size of two-loop corrections. We will also compare our results with previous two-loop calculations [4, 7].

The rest of the paper is organized as follows: We first present a general formalism for calculating the CP -even Higgs-boson mass from the effective potential in Section 2, and compute the two-loop effective potential to the order of $\mathcal{O}(\lambda_t^2 \alpha_s)$. We next show the results of our numerical analyses in Section 3; we find good agreements with

previous two-loop calculations. Finally we conclude in Section 4. For completeness, some functions which appear in the two-loop calculation are given in the Appendix.

2 Effective Potential and the CP -even Higgs-boson Masses

We start our analysis with the tree-level potential of the MSSM[†],

$$V_{\text{tree}} = (m_{H_1}^2 + \mu^2)|H_1|^2 + (m_{H_2}^2 + \mu^2)|H_2|^2 + \mu B(H_1 H_2 + \text{H.c.}) + \frac{g^2 + g'^2}{8}(|H_1|^2 - |H_2|^2)^2 + \frac{g^2}{2}|H_1^\dagger H_2|^2, \quad (1)$$

where g, g' are the $SU(2)$ and $U(1)_Y$ gauge couplings, m_{H_1}, m_{H_2} and B are the soft-breaking Higgs-sector mass parameters, and μ is the supersymmetric Higgs-boson mass parameter (the μ -parameter).

We express H_1 and H_2 in terms of their component fields,

$$H_1 = \begin{pmatrix} (S_1 + iP_1)/\sqrt{2} \\ H_1^- \end{pmatrix}, \quad H_2 = \begin{pmatrix} H_2^+ \\ (S_2 + iP_2)/\sqrt{2} \end{pmatrix}, \quad (2)$$

so the tree-level potential can be rewritten as a function of the CP -even fields, S_1 and S_2 . In general, the all-loop effective potential is a function of S_1 and S_2 , which are usually known as classical fields.

The technique for calculating a higher loop effective potential was developed long ago by Jackiw [9]. First, the Higgs fields are expanded around the classical fields, in terms of which all the relevant particle masses and couplings are determined. One then calculates the higher loop effective potential by computing the corresponding zero-point function Feynman diagrams (bubble diagrams).

To be more specific, to the two-loop order that we consider in this paper, we write the effective potential as

$$V(S_1, S_2) = V_0 + V_{\text{tree}}(S_1, S_2) + V_{1\text{loop}}(S_1, S_2) + V_{2\text{loop}}(S_1, S_2), \quad (3)$$

where V_0 is a field-independent vacuum-energy term, and $V_{\text{tree}}, V_{1\text{loop}}$ and $V_{2\text{loop}}$ are the tree-level, one- and two-loop contributions respectively. V_0 is necessary for the renormalization group invariance of the effective potential [10].

The one-loop effective potential in the $\overline{\text{DR}}$ scheme is well-known. It can be easily obtained by calculating the one-loop bubble diagrams with all kinds of (s)particles running in the loop. We find that in the Landau gauge

$$V_{1\text{loop}}(S_1, S_2) = \sum_f \sum_{i=1}^2 N_c^f G(\tilde{f}_i) - 2 \sum_f N_c^f G(f) + 3G(W) + \frac{3}{2}G(Z)$$

[†]We work in the modified $\overline{\text{DR}}$ -scheme of Ref. [8].

$$\begin{aligned}
& + \frac{1}{2} \left[G(H) + G(h) + G(A) + G(G) \right] + G(H^+) + G(G^+) \\
& - 2 \sum_{i=1}^2 G(\tilde{\chi}_i^+) - \sum_{i=1}^4 G(\tilde{\chi}_i^0), \tag{4}
\end{aligned}$$

where f sums over all the (s)quarks and (s)leptons, N_c^f is the color factor, 3 for (s)quarks and 1 for (s)leptons, and all the masses are implicitly S_1 , S_2 -dependent. H , h , A and G (H^+ and G^+) label the neutral (charged) Higgs and Goldstone bosons, $\tilde{\chi}_i^+$ and $\tilde{\chi}_i^0$ represent charginos and neutralinos. We have also used short-handed notations $f_i = m_{\tilde{f}_i}^2$, $W = m_W^2$, etc. The function $G(x)$ is defined as

$$G(x) = \frac{x^2}{32\pi^2} \left(\overline{\ln} x - \frac{3}{2} \right), \tag{5}$$

where $\overline{\ln} x = \ln(x/Q^2)$, with Q the renormalization scale.

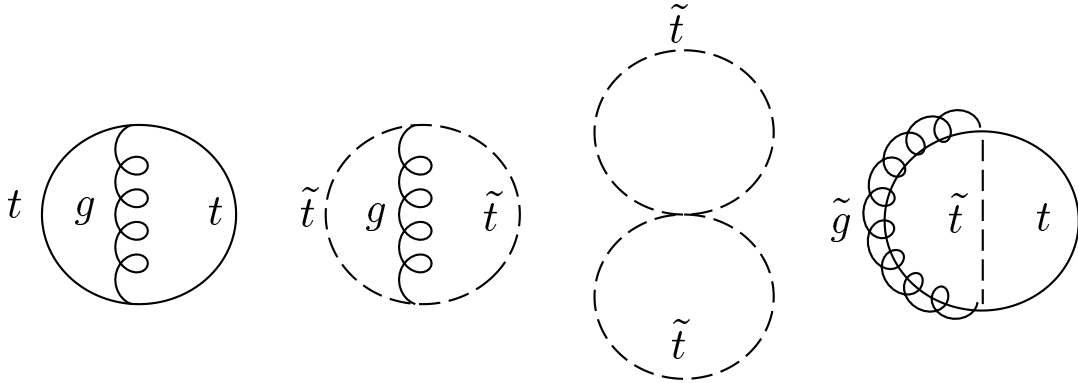


Figure 1: Bubble diagrams for the two-loop effective potential to the order of $\mathcal{O}(\lambda_t^2 \alpha_s)$ in the MSSM.

The two-loop effective potential can be derived similarly, the corresponding Feynman diagrams are plot in Fig. 1. To the order of $\mathcal{O}(\lambda_t^2 \alpha_s)$, we have in the Landau gauge

$$\begin{aligned}
V_{2\text{loop}}(S_1, S_2) = & 32\pi\alpha_s \left\{ J(t, t) - 2t I(t, t, 0) \right. \\
& + \frac{1}{2} (c_t^4 + s_t^4) \sum_{i=1}^2 J(\tilde{t}_i, \tilde{t}_i) + 2s_t^2 c_t^2 J(\tilde{t}_1, \tilde{t}_2) + \sum_{i=1}^2 \tilde{t}_i I(\tilde{t}_i, \tilde{t}_i, 0) \\
& \left. + \sum_{i=1}^2 L(\tilde{t}_i, \tilde{g}, t) - 4m_{\tilde{g}} m_t s_t c_t \left(I(\tilde{t}_1, \tilde{g}, t) - I(\tilde{t}_2, \tilde{g}, t) \right) \right\} \tag{6}
\end{aligned}$$

where the (minimally) subtracted functions I and J are defined in the Appendix, s_t is the top-squark mixing angle. This effective potential, in the limit of $\tan \beta \rightarrow \infty$ and

no left-right squark-mixing ($s_t = 0$), agrees with that of Ref. [6]. As a good check, one can show that the effective potential $V(S_1, S_2)$ is invariant under the renormalization scale change, up to two-loop terms which are ignored in our approximation.

The effective potential Eq. (6), as a generating functional, encodes the information of two-loop tadpoles and self-energies at zero external momentum. From this, one can find two-loop CP -even Higgs-boson masses by solving appropriate on-mass-shell conditions.

This proceeds as follows: We first minimize $V(S_1, S_2)$ at the Higgs vacuum expectation values $S_1 = v_1$ and $S_2 = v_2$,

$$\left. \frac{\partial V}{\partial S_1} \right|_{S_1=v_1, S_2=v_2} = 0, \quad \left. \frac{\partial V}{\partial S_2} \right|_{S_1=v_1, S_2=v_2} = 0, \quad (7)$$

which is equivalent to the requirement that the tadpoles vanish,

$$\frac{T_1}{v_1} = \frac{1}{2}m_Z^2 c_{2\beta} + m_{H_1}^2 + \mu^2 + B\mu \tan \beta, \quad (8)$$

$$\frac{T_2}{v_2} = -\frac{1}{2}m_Z^2 c_{2\beta} + m_{H_2}^2 + \mu^2 + B\mu \cot \beta, \quad (9)$$

where $\tan \beta = v_2/v_1$, $m_Z^2 = (g^2 + g'^2)v^2/4$ and $v^2 = v_1^2 + v_2^2$. To the two-loop order, the tadpoles $T_i, i = 1, 2$ are given by $T_i = T_i^{\text{1loop}} + T_i^{\text{2loop}}$, where the one- and two-loop tadpoles are defined by

$$T_i^{\text{1loop}} = -\left(\frac{\partial V_{\text{1loop}}}{\partial S_i} \right) \Big|_{S_1=v_1, S_2=v_2}, \quad T_i^{\text{2loop}} = -\left(\frac{\partial V_{\text{2loop}}}{\partial S_i} \right) \Big|_{S_1=v_1, S_2=v_2}. \quad (10)$$

One can check that the one-loop tadpoles T_i^{1loop} obtained in this way give the same results as in Ref. [11][‡], where they were explicitly calculated from the one-point function Feynman diagrams (tadpole diagrams).

The CP -even Higgs-boson mass matrix, after some algebra, is

$$\mathcal{M}^2(p^2) = \begin{pmatrix} m_Z^2 c_\beta^2 + m_A^2 s_\beta^2 - \text{Re}\Pi_{11}(p^2) + T_1/v_1 & -(m_Z^2 + m_A^2)s_\beta c_\beta - \text{Re}\Pi_{12}(p^2) \\ -(m_Z^2 + m_A^2)s_\beta c_\beta - \text{Re}\Pi_{12}(p^2) & m_Z^2 s_\beta^2 + m_A^2 c_\beta^2 - \text{Re}\Pi_{22}(p^2) + T_2/v_2 \end{pmatrix}, \quad (11)$$

where $m_A^2 = -\mu B(\tan \beta + \cot \beta)$, and both m_Z and m_A are $\overline{\text{DR}}$ running masses. Π 's represent two-point functions (self-energies).

The radiatively corrected Higgs-boson masses can be found by computing the zeroes of the inverse propagator, $p^2 - \mathcal{M}^2(p^2)$. The complete one-loop formulae for

[‡]In Ref. [11], we used the 't Hooft-Feynman gauge. To compare with the one-loop tadpoles obtained from Eq. (4), the Goldstone boson masses need to be set to zero.

self-energies at nonzero external momentum can be found, *e.g.* in Ref. [11]. For the two-loop self-energies, we shall approximate them as follows:

$$\Pi_{ij}^{2\text{loop}}(0) = -\left(\frac{\partial^2 V_{2\text{loop}}}{\partial S_i \partial S_j}\right)\Big|_{S_1=v_1, S_2=v_2}, \quad i, j = 1, 2. \quad (12)$$

The difference of $\Pi_{ij}^{2\text{loop}}(0)$ and $\Pi_{ij}^{2\text{loop}}(p^2)$ is negligible.

3 Numerical Procedure and Results

We shall first show the improvement of renormalization scale (Q) dependence of the lightest CP -even Higgs-boson mass. We start by solving the two-loop renormalization group equations (RGEs) of the MSSM. The boundary condition inputs for these RGEs are taken to be the observables α_s , α_{em} , G_F , M_Z , m_t , m_b and m_τ at the electro-weak scale, M_Z , and the universal scalar soft mass M_0 , gaugino soft mass $M_{1/2}$ and trilinear scalar coupling A_0 at the unification scale, $M_{\text{GUT}} \approx 2 \times 10^{16}$ GeV (This is sometimes called the minimal supergravity (mSUGRA) scenario.). We have also properly taken into account the low energy threshold corrections to the gauge and Yukawa couplings, as in Ref. [11].

In this scenario, the μ -parameter and the (tree-level) mass m_A are determined in terms of other variables through the minimization conditions (8) and (9), which ensure the correct electro-weak symmetry breaking,

$$\mu^2 = \frac{1}{2} \left[\tan 2\beta \left(\overline{m}_{H_2}^2 \tan \beta - \overline{m}_{H_1}^2 \cot \beta \right) - m_Z^2 \right], \quad (13)$$

$$m_A^2 = \frac{1}{\cos 2\beta} \left(\overline{m}_{H_2}^2 - \overline{m}_{H_1}^2 \right) - m_Z^2, \quad (14)$$

where $\overline{m}_{H_1}^2 = m_{H_1}^2 - T_1/v_1$ and $\overline{m}_{H_2}^2 = m_{H_2}^2 - T_2/v_2$.

We then calculate the lightest CP -even Higgs-boson mass from the mass-squared matrix Eq. (11). We use the one-loop tadpole and self-energy formulae from Ref. [11], while for the two-loop contributions, we compute the tadpoles and self-energies numerically according to Eqs. (10) and (12) by replacing the differentiation by a finite difference. The field-dependent masses in Eq. (6) are the top-quark mass $m_t = \lambda_t S_2 / \sqrt{2}$ and the top-squark masses which are found from the following field-dependent mass-squared matrix:

$$\begin{pmatrix} M_Q^2 + \frac{1}{2} \lambda_t^2 S_2^2 & \frac{1}{\sqrt{2}} \lambda_t (A_t S_2 + \mu S_1) \\ \frac{1}{\sqrt{2}} \lambda_t (A_t S_2 + \mu S_1) & M_U^2 + \frac{1}{2} \lambda_t^2 S_2^2 \end{pmatrix}, \quad (15)$$

where we have neglected the field-dependent D -term contributions and M_Q, M_U are squark soft masses at the low-energy scale. The field-dependent angle s_t in Eq. (6) is defined as the mixing angle of the above mass-squared matrix.

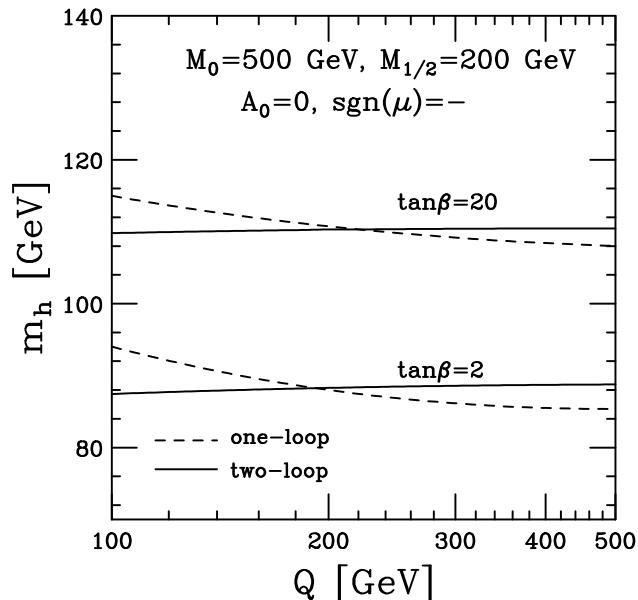


Figure 2: Renormalization-scale (Q) dependence of the lightest CP -even Higgs-boson mass m_h . The dashed and solid lines correspond to the one- and two-loop masses respectively. We have fixed the universal boundary conditions, $M_0 = 500$ GeV, $M_{1/2} = 200$ GeV, $A_0 = 0$, and chosen a negative μ -parameter.

In Fig. 2, we show the dependence of one- and two-loop radiatively corrected CP -even Higgs-boson masses m_h on the renormalization scale Q . We choose the universal soft parameters $M_0 = 500$ GeV, $M_{1/2} = 200$ GeV and $A_0 = 0$ at the unification scale, and set the sign of μ -parameter to be negative[§]. We plot two choices of $\tan\beta$, 2 and 20. The one- and two-loop masses are shown in dashed and solid lines respectively. In the corrections to the Higgs-boson masses m_h , we have used the $\overline{\text{DR}}$ running top-Yukawa coupling at the scale Q . The formulae which convert the top-quark pole mass m_t^{pole} to $\lambda_t(Q)$ are given in Ref. [11].

We see that the one-loop radiatively corrected Higgs-boson masses vary by about 10 GeV as the renormalization scale Q varies from 100 to 500 GeV. However, once we properly include the two-loop radiative corrections, the scale dependence of m_h becomes much milder, and we find for all ranges of the scale $m_h \simeq 88$ GeV and 110 GeV for $\tan\beta = 2$ and 20 respectively. The two-loop calculation can only change m_h by a few GeV.

In Figs. 3 and 4, we compare our results with that of RGE-improved effective potential (EP) approach [4]. In that approach, the heavy particles are decoupled at $m_{\tilde{t}}$ (or $m_{\tilde{t}_1}$ and $m_{\tilde{t}_2}$ stepwisely if they are very different). The two-loop RGEs of the effective field theory below the decoupling scale is then used to run the effective couplings to the scale where the Higgs-boson mass is evaluated, *e.g.* the on-shell top-

[§]Our convention of the sign of μ -parameter is opposite to that of Refs. [4] and [7].

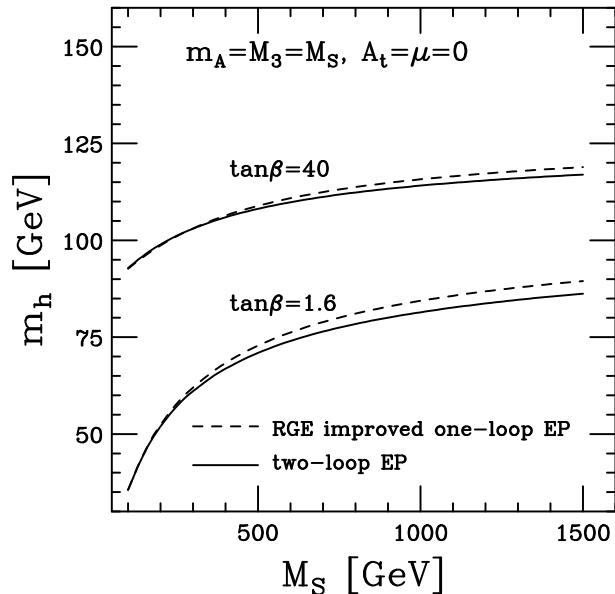


Figure 3: Higgs boson masses m_h vs. the squark soft masses M_S in the no-squark-mixing case $A_t = \mu = 0$. The solid lines are results from the two-loop EP approach. For comparison, we also show the results from the RGE-improved one-loop EP approach in dashed lines.

quark mass. Since the next-to-leading-order corrections are negligible at this scale [3], this allows an analytical solution to the two-loop RGEs [4].

In this part of numerical analysis, we do not impose the minimization conditions Eqs. (8) and (9), instead, the μ -parameter and the CP -odd Higgs boson mass m_A are taken as inputs. We further choose the squark soft masses $M_Q = M_U = M_S$. In Fig. 3, we show the two-loop Higgs-boson masses m_h versus M_S , in the RGE-improved one-loop EP approach (dashed lines) and in the two-loop EP approach (solid lines). The parameters A_t and μ are set to zero; this corresponds to the no left-right squark-mixing limit. Other parameters are $m_A = M_3 = M_S$. Results from the two approaches generally agree to $\lesssim 3$ GeV, for both small and large $\tan\beta$ cases. The difference comes from the $\mathcal{O}(\lambda_t^4)$ corrections which are neglected in this calculation [7].

In Fig. 4, we choose a nonzero μ -parameter, $\mu = -200$ GeV, and plot m_h versus X_t/M_S , where $X_t = A_t + \mu/\tan\beta$ is related to the off-diagonal element of the squark-mass matrix. We see the results from the two approaches still agree quite well except for the large X_t/M_S . In particular, the curves for the two-loop EP approach peak at $X_t/M_S \simeq \pm 2$, which is different from the RGE-improved one-loop EP approach. This however agrees with the results of a recent analysis [7]. The slight asymmetry of the solid curves with respect to the reflection, $X_t \rightarrow -X_t$, originates from the last term in Eq. (6). We found that for $\tan\beta = 40$ the upper limit for the Higgs-boson mass is 125 GeV at the large squark-mixing ($X_t/M_S = \pm 2$).

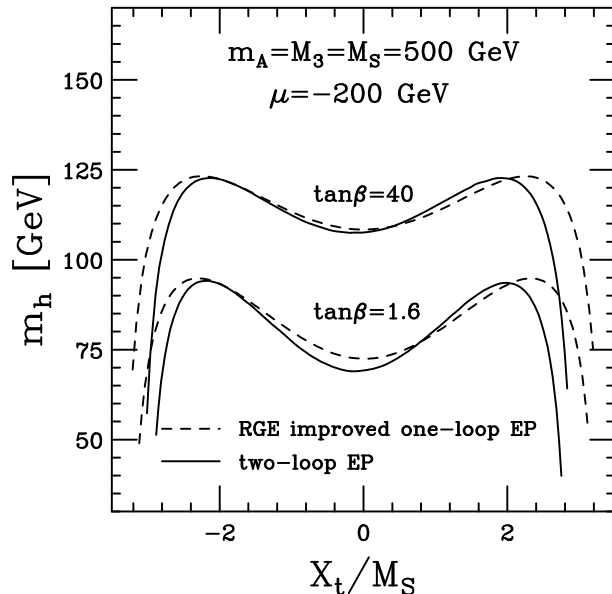


Figure 4: Higgs-boson masses m_h vs. X_t/M_S , where $X_t = A_t + \mu/\tan\beta$. Both the results from the RGE-improved one-loop EP and two-loop EP approaches are shown.

4 Conclusions

To conclude, we have used an effective potential method to calculate the two-loop corrections to the lightest CP -even Higgs-boson mass in the MSSM. Our approach is straightforward and easy to program, and can be extended to include two-loop corrections of order $\mathcal{O}(\lambda_t^4)$. We show that the renormalization scale dependence of m_h improves after including the two-loop corrections, this largely reduces the uncertainty associated with one-loop calculations. We have shown that the two-loop correction is only about a few GeV with respect to the one-loop results (where the $\overline{\text{DR}}$ running coupling λ_t is used). We have also compared our results with some previous two-loop calculations. We found good agreements with the RGE-improved one-loop EP approach of Ref. [4] except for the case of large left-right squark mixing, where we obtained similar results as in Ref. [7]. The upper bound for the Higgs-boson mass $m_h \lesssim 125$ GeV is achieved at the region of parameter space for large $\tan\beta$ and left-right squark mixings.

Acknowledgements

I would like to thank K. Matchev for participating in the early stage of this work, J. Bagger, T. Han and C. Kao for conversations and comments, and C. Wagner and G. Weiglein for communications and numerical comparisons. This work was supported

in part by a DOE grant No. DE-FG02-95ER40896 and in part by the Wisconsin Alumni Research Foundation.

Appendix: The functions $I(x, y, z)$ and $J(x, y)$

Momentum integrals arising from the two-loop bubble diagrams have one-loop subdivergences which can be subtracted in the standard way [12]. Furthermore, in the $\overline{\text{DR}}$ scheme there is no complication associated with vector-boson loops[¶], so all integrals can be expressed in terms of (minimally) subtracted functions I , J which are [12]

$$(16\pi^2)^2 J(x, y) = x y \left[1 - \overline{\ln} x - \overline{\ln} y + \overline{\ln} x \overline{\ln} y \right], \quad (\text{A.1})$$

$$(16\pi^2)^2 I(x, y, z) = -\frac{1}{2} \left[(y + z - x) \overline{\ln} y \overline{\ln} z + (z + x - y) \overline{\ln} z \overline{\ln} x \right. \\ \left. + (x + y - z) \overline{\ln} x \overline{\ln} y - 4(x \overline{\ln} x + y \overline{\ln} y + z \overline{\ln} z) + \xi(x, y, z) + 5(x + y + z) \right], \quad (\text{A.2})$$

where ξ is given by

$$\xi(x, y, z) = 8b \left[L(\theta_x) + L(\theta_y) + L(\theta_z) - \frac{\pi}{2} \ln 2 \right] \quad (\text{A.3})$$

when $-b^2 = a^2 = (x^2 + y^2 + z^2 - 2xy - 2xz - 2yz)/4 \leq 0$, and

$$\xi(x, y, z) = 8a \left[-M(-\phi_x) + M(\phi_y) + M(\phi_z) \right] \quad (\text{A.4})$$

when $a^2 > 0$. Here $L(t)$ is Lobachevsky's function, defined as

$$L(t) = -\int_0^t dx \ln \cos x = t \ln 2 - \frac{1}{2} \sum_{k=1}^{\infty} (-)^{k-1} \frac{\sin 2kt}{k^2}, \quad (\text{A.5})$$

and the function $M(t)$ is defined as

$$M(t) = -\int_0^t dx \ln \sinh x = \frac{\pi^2}{12} - \frac{t^2}{2} + t \ln 2 - \frac{1}{2} \text{Li}_2(e^{-2t}), \quad (\text{A.6})$$

Li_2 is the dilogarithm function.

The angles $\theta_{x,y,z}$ and $\phi_{x,y,z}$ are defined by

$$\theta_x = \arctan\left(\frac{y+z-x}{2b}\right), \quad \phi_x = \text{arccoth}\left(\frac{y+z-x}{2a}\right), \quad \text{etc.} \quad (\text{A.7})$$

Finally we have also used the following function in the two-loop effective potential:

$$L(x, y, z) = J(y, z) - J(x, y) - J(x, z) - (x - y - z)I(x, y, z). \quad (\text{A.8})$$

[¶]In contrast, the vector bosons live in $d = 4 - 2\epsilon$ dimensions in the $\overline{\text{MS}}$ scheme, in reducing the two-loop integrals to the form of I and J , there will be extra finite terms from themselves and the associated one-loop subdiagrams.

References

- [1] S.P. Li and M. Sher, Phys. Lett. **B140** (1984) 339; Y. Okada, M. Yamaguchi, and T. Yanagida, Prog. Theor. Phys. **85** (1991) 1; Phys. Lett. **B262** (1991) 54; J. Ellis, G. Ridolfi and F. Zwirner, Phys. Lett. **B257** (1991) 83; H.E. Haber and R. Hempfling, Phys. Rev. Lett. **66** (1991) 1815; R. Barbieri, M. Frigeni and M. Caravaglios, Phys. Lett. **B263** (1991) 233; P.H. Chankowski, preprint IFT-7-91-WARSAW (1991); J.R. Espinosa and M. Quiros, Phys. Lett. **B266** (1991) 389; J.L. Lopez and D.V. Nanopoulos, Phys. Lett. **B266** (1991) 397; D.M. Pierce, A. Papadopoulos and S.B. Johnson, Phys. Rev. Lett. **68** (1992) 3678; A. Brignole, Phys. Lett. **B281** (1992) 284; P.H. Chankowski, S. Pokorski and J. Rosiek, Nucl. Phys. **B423** (1994) 437; A. Dabelstein, Z. Phys. **C67** (1995) 495.
- [2] J. Kodaira, Y. Yasui and K. Sasaki, Phys. Rev. **D50** (1994) 7035; A.V. Gladyshev and D.I. Kazakov, Mod. Phys. Lett. **A10** (1995) 3129; M. Carena, J.R. Espinosa, M. Quiros and C.E.M. Wagner, Phys. Lett. **B355** (1995) 209.
- [3] J.A. Casas, J.R. Espinosa, M. Quiros and A. Riotto, Nucl. Phys. **B436** (1995) 3.
- [4] M. Carena, M. Quiros and C.E.M. Wagner, Nucl. Phys. **B461** (1996) 407.
- [5] H.E. Haber, in *Brussels EPS HEP 1995*, hep-ph/9601330; H.E. Haber, R. Hempfling and A. Hoang, Z. Phys. **C75** (1997) 539.
- [6] R. Hempfling and A.H. Hoang, Phys. Lett. **B331** (1994) 99.
- [7] S. Heinemeyer, W. Hollik and G. Weiglein, hep-ph/9803277; hep-ph/9807423.
- [8] I. Jack, D.R.T. Jones, S.P. Martin, M.T. Vaughn and Y. Yamada, Phys. Rev. **D50** (1994) 5481.
The original \overline{DR} scheme was discussed in
W. Siegel, Phys. Lett. **B84** (1979) 193; D.M. Capper, D.R.T. Jones and P. van Nieuwenhuizen, Nucl. Phys. **B167** (1980) 479.
- [9] R. Jackiw, Phys. Rev. **D9** (1974) 1686.
- [10] B. Kastening, Phys. Lett. **B283** (1992) 287.
- [11] D.M. Pierce, J.A. Bagger, K.T. Matchev and R.-J. Zhang, Nucl. Phys. **B491** (1997) 3.
- [12] C. Ford and D.R.T. Jones, Phys. Lett. **B274** (1992) 409; C. Ford, I. Jack and D.R.T. Jones, Nucl. Phys. **B387** (1992) 373.